Neutrino Interferometry for High-Precision Tests of Lorentz Symmetry with IceCube

C. Argüelles on behalf of the IceCube collaboration

Abstract: Lorentz symmetry is a fundamental space-time symmetry underlying both the Standard Model of particle physics and general relativity. This symmetry guarantees that physical phenomena are observed to be the same by all inertial observers. However, unified theories, such as string theory, allow for violation of this symmetry by inducing new space-time structure at the quantum gravity scale. Thus, the discovery of Lorentz symmetry violation (LV) could be the first hint of these theories in Nature. Here we report the results of the most precise test of space-time symmetry in the neutrino sector to date. We use high-energy atmospheric neutrinos observed at the IceCube Neutrino Observatory to search for anomalous neutrino oscillations as signals of Lorentz violation. We find no evidence for such phenomena. This allows us to constrain the size of the dimension-four operator in the Standard-Model Extension (SME) for Lorentz violation to the 10^{-28} level and to set limits on higher dimensional operators in this framework. These are among the most stringent limits on Lorentz violation set by any physical experiment.

Lorentz Violation in the Standard-Model Extension (SME)

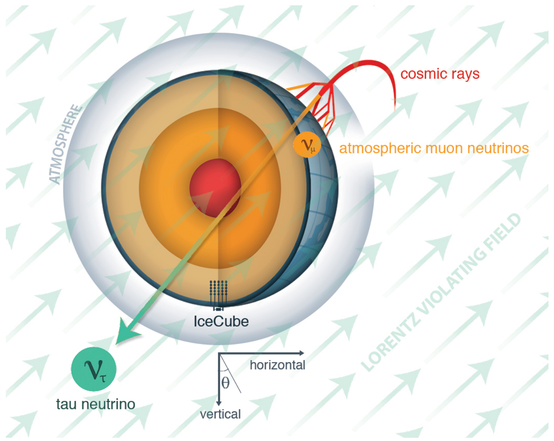

Figure 1: Cartoon shows the idea of this analysis, namely that atmospheric muon neutrinos disappearances is induced by the Lorentz violating field potential.

The LV effect can be introduced in the neutrino Hamiltonian as follows

$$H \sim \frac{m^2}{2E} + \mathring{a}^{(3)} - E \cdot \mathring{c}^{(4)} + E^2 \cdot \mathring{a}^{(5)} - E^3 \cdot \mathring{c}^{(6)} \cdots$$

where circle denotes that we are considering only time-independent isotropic LV fields and the “a” terms are CPT-odd while “c" terms are CPT-even coefficient. The numbers in parentheses denote the operator dimension.

Since at high-energies matter effects overwhelm possible LV-induced transition between electron neutrinos and the other flavors, we restrict ourselves to a two-flavor system. Thus each term, “a” or “c”, is given by a 2x2 hermitian matrix. We also define the *strength* of LV as

$$\rho_d \equiv \sqrt{(\mathring{c}^{(d)}_{\mu\mu})^2 + \mathrm{Re}\,(\mathring{c}^{(d)}_{\mu\tau})^2 + \mathrm{Im}\,(\mathring{c}^{(d)}_{\mu\tau})^2}$$

Explicit form of dimension-6 term:

$$\mathring{c}^{(6)} = \begin{pmatrix} \mathring{c}^{(6)}_{\mu\mu} & \mathring{c}^{(6)}_{\mu\tau} \\ \mathring{c}^{(6)*}_{\mu\tau} & -\mathring{c}^{(6)}_{\mu\mu} \end{pmatrix}$$

Dataset and systematics

Figure 2: This analysis uses up-going muon neutrinos collected over a two year period. The figure shows the muon energy distribution of this sample [1]. We restrict ourselves to energies less than 18 TeV and more than 400 GeV. In this range we have 34975 events. In this sample atmospheric muon contamination is less than 1%.

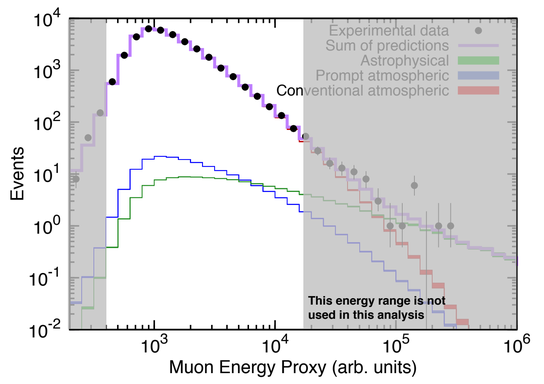

Systematics: We introduce six systematic parameters related to the neutrino flux prediction: normalizations of conventional (40% error), prompt (no constraint), and astrophysical (no constraint) neutrino flux components; ratio of pion and kaon contributions for conventional flux (10% error); spectral index of primary cosmic rays (2% error); and astrophysical neutrino spectral index (25% error). The impact of light propagation model uncertainties on the horizontal to vertical ratio is less than 5% at a few TeV, and the overall efficiency of the detector is controlled by the energy distribution peak. For this measurement, these latter uncertainties are sub-leading with respect to the flux uncertainties we consider.

Result for dimension six operator

Figure 3: The left panel shows the ratio of the vertical to horizontal transition probabilities as a function of energy. The solid color lines show the effect of LV dimension six operator. The transition probability increases with energy and length, which causes a deficit of vertical events. This translates to an exclusion shown in the right panel. This is limited on the left by finite statistics, on the right by absolute normalization of the atmospheric flux, and in the top and bottom white regions have suppressed transition probability.

$$P(\nu_\mu \to \nu_\tau) \sim \left(\frac{\mathring{a}^{(d)}_{\mu\tau} - \mathring{c}^{(d)}_{\mu\tau}}{\rho_d} \right)^2 \sin^2(L\rho_d \cdot E^{d-3})$$

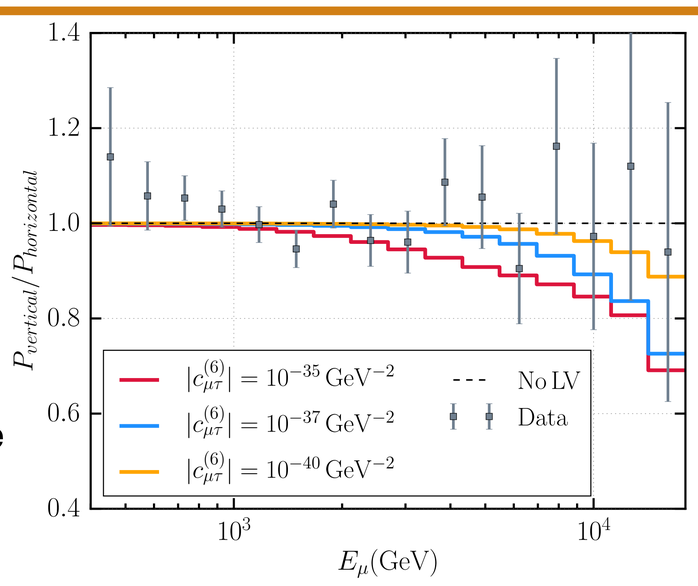

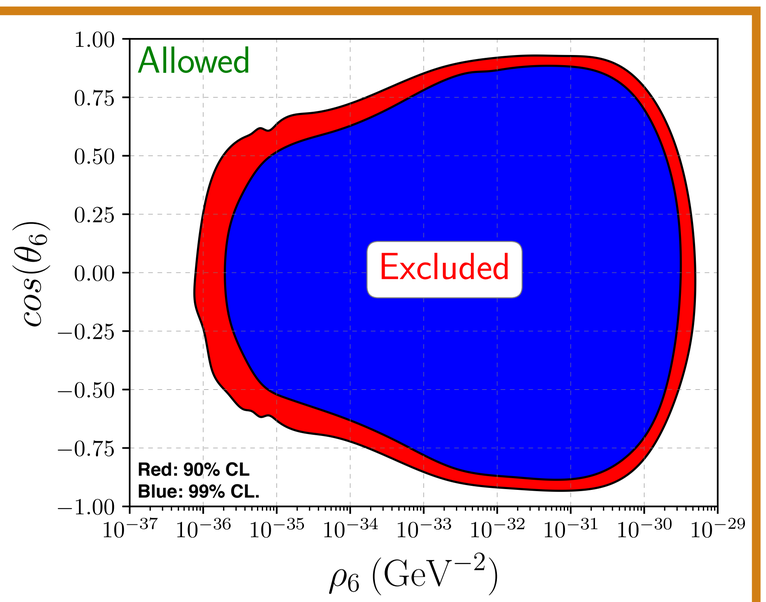

New constraints on Lorentz Violating operations assuming maximal flavor violation

Figure 4: Each panel shows the constraints on LV operators for a given dimension from three to eight. The red and blue colors denote 90% and 99% C.L. exclusion, respectively. Maximal flavor violation is setting the diagonal terms to zero.

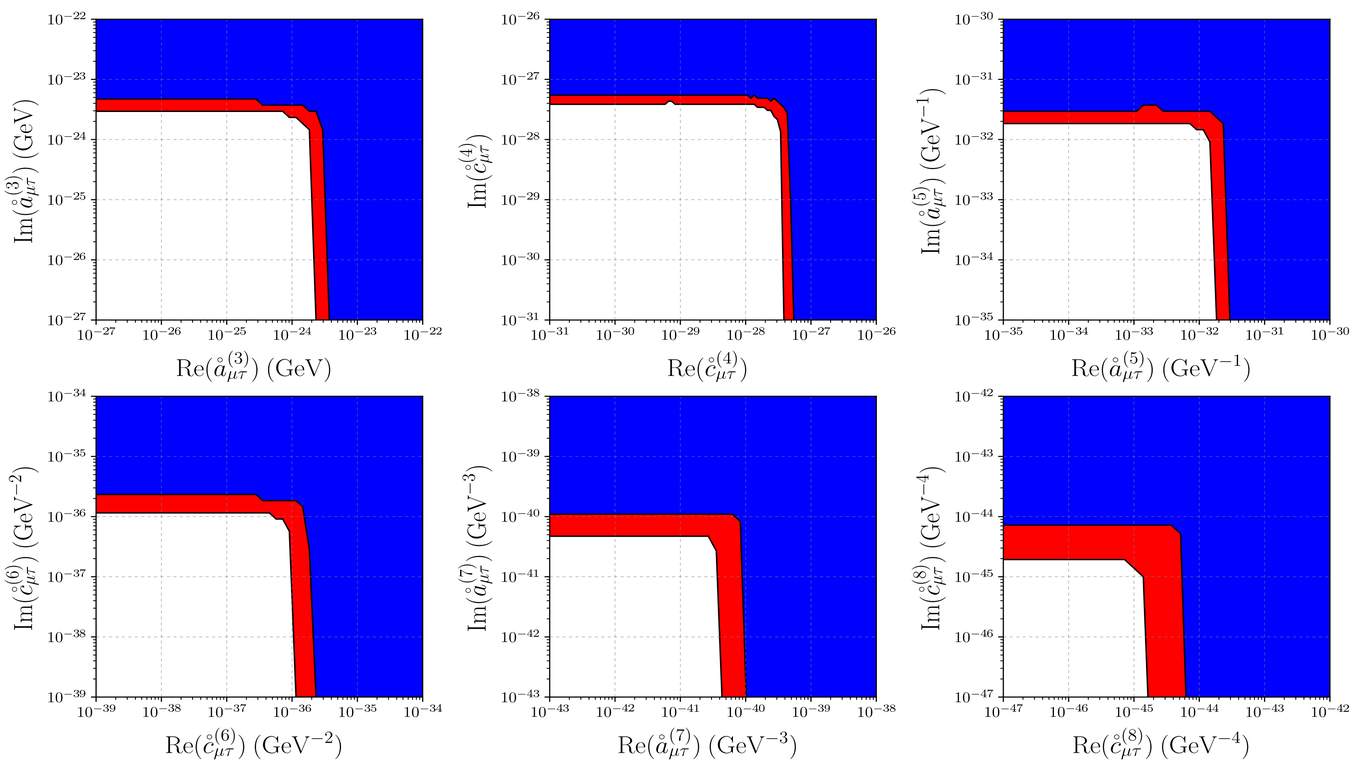

Comparison with other SME sectors

dim.	method	type	sector	limits	
3	CMB polarization	astrophysical	photon	$\sim 10^{-43}$ GeV	[2]
	He-Xe comagnetometer	tabletop	neutron	$\sim 10^{-34}$ GeV	[3]
	torsion pendulum	tabletop	electron	$\sim 10^{-31}$ GeV	[4]
	muon g-2	accelerator	muon	$\sim 10^{-24}$ GeV	[5]
	neutrino oscillation	atmospheric	neutrino	$\lvert\mathrm{Re}\,(\mathring{a}^{(3)}_{\mu\tau})\rvert, \lvert\mathrm{Im}\,(\mathring{a}^{(3)}_{\mu\tau})\rvert$ $< 2.9 \times 10^{-24}$ GeV (99% C.L.) $< 2.0 \times 10^{-24}$ GeV (90% C.L.)	
4	GRB vacuum birefringence	astrophysical	photon	$\sim 10^{-38}$	[6]
	Laser interferometer	LIGO	photon	$\sim 10^{-22}$	[7]
	Sapphire cavity oscillator	tabletop	photon	$\sim 10^{-18}$	[8]
	Ne-Rb-K comagnetometer	tabletop	neutron	$\sim 10^{-29}$	[9]
	trapped Ca^+ ion	tabletop	electron	$\sim 10^{-19}$	[10]
	neutrino oscillation	atmospheric	neutrino	$\lvert\mathrm{Re}\,(\mathring{c}^{(4)}_{\mu\tau})\rvert, \lvert\mathrm{Im}\,(\mathring{c}^{(4)}_{\mu\tau})\rvert$ $< 3.9 \times 10^{-28}$ (99% C.L.) $< 2.7 \times 10^{-28}$ (90% C.L.)	
5	GRB vacuum birefringence	astrophysical	photon	$\sim 10^{-34}$ GeV^{-1}	[6]
	ultra-high-energy cosmic ray	astrophysical	proton	$\sim 10^{-22}$ to 10^{-18} GeV^{-1}	
	neutrino oscillation	atmospheric	neutrino	$\lvert\mathrm{Re}\,(\mathring{a}^{(5)}_{\mu\tau})\rvert, \lvert\mathrm{Im}\,(\mathring{a}^{(5)}_{\mu\tau})\rvert$ $< 2.3 \times 10^{-32}$ GeV^{-1} (99% C.L.) $< 1.5 \times 10^{-32}$ GeV^{-1} (90% C.L.)	
6	GRB vacuum birefringene	astrophysical	photon	$\sim 10^{-31}$ GeV^{-2}	[6]
	ultra-high-energy cosmic ray	astrophysical	proton	$\sim 10^{-42}$ to 10^{-35} GeV^{-2}	[11]
	gravitational Cherenkov radiation	astrophysical	gravity	$\sim 10^{-31}$ GeV^{-2}	
	neutrino oscillation	atmospheric	neutrino	$\lvert\mathrm{Re}\,(\mathring{c}^{(6)}_{\mu\tau})\rvert, \lvert\mathrm{Im}\,(\mathring{c}^{(6)}_{\mu\tau})\rvert$ $< 1.5 \times 10^{-36}$ GeV^{-2} (99% C.L.) $< 9.1 \times 10^{-37}$ GeV^{-2} (90% C.L.)	
7	GRB vacuum birefringence	astrophysical	photon	$\sim 10^{-28}$ GeV^{-3}	[6]
	neutrino oscillation	atmospheric	neutrino	$\lvert\mathrm{Re}\,(\mathring{a}^{(7)}_{\mu\tau})\rvert, \lvert\mathrm{Im}\,(\mathring{a}^{(7)}_{\mu\tau})\rvert$ $< 8.3 \times 10^{-41}$ GeV^{-3} (99% C.L.) $< 3.6 \times 10^{-41}$ GeV^{-3} (90% C.L.)	
8	gravitational Cherenkov radiation	astrophysical	gravity	$\sim 10^{-46}$ GeV^{-4}	
	neutrino oscillation	atmospheric	neutrino	$\lvert\mathrm{Re}\,(\mathring{c}^{(8)}_{\mu\tau})\rvert, \lvert\mathrm{Im}\,(\mathring{c}^{(8)}_{\mu\tau})\rvert$ $< 5.2 \times 10^{-45}$ GeV^{-4} (99% C.L.) $< 1.4 \times 10^{-45}$ GeV^{-4} (90% C.L.)	

Table 1: Each row contains a summary of constraints on the SME coefficients for a given dimension. The penguin marker signals the results of this analysis. The lower dimension operators are dominated by photon observations, whereas the higher dimensions are dominated by neutrinos and gravity. It's notable that this work is among the strongest constraints on dimension six operators.

References:

1. Evidence for Astrophysical Muon Neutrinos from the Northern Sky with IceCube - IceCube Collaboration (Aartsen, M.G. et al.) Phys.Rev.Lett. 115 (2015) no.8, 081102
2. E. Komatsu et al. [WMAP Collaboration], “Five-Year Wilkinson Microwave Anisotropy Probe (WMAP) Observations: Cosmological Interpretation,” Astrophys. J. Suppl. 180, 330-376 (2009).
3. F. Allmendinger et al., “New Limit on Lorentz-Invariance- and CPT-Violating Neutron Spin Interactions Using a Free- Spin-Precession ^{3}He - ^{129}Xe Comagnetometer,” Phys. Rev. Lett. 112, no. 11, 110801 (2014).
4. B. R. Heckel et al., “New CP-violation and preferred-frame tests with polarized electrons,” Phys. Rev. Lett. 97, 021603 (2006).
5. G. W. Bennett et al. [Muon (g-2) Collaboration], “Search for Lorentz and CPT violation effects in muon spin precession,” Phys. Rev. Lett. 100, 091602 (2008).
6. V. A. Kostelecky´ and M. Mewes, “Constraints on relativity violations from gamma-ray bursts,” Phys. Rev. Lett. 110, no. 20, 201601 (2013).
7. V. A. Kostelecky´, A. C. Melissinos and M. Mewes, “Searching for photon-sector Lorentz violation using gravitational-wave detectors,” Phys. Lett. B 761, 1-7 (2016).
8. M. Nagel et al., “Direct Terrestrial Test of Lorentz Symmetry in Electrodynamics to 10^{-18},” Nature Commun. 6, 8174 (2015).
9. M. Smiciklas, J. M. Brown, L. W. Cheuk and M. V. Romalis, “A new test of local Lorentz invariance using ^{21}Ne-Rb-K comagnetometer,” Phys. Rev. Lett. 107, 171604 (2011).
10. V. A. Kostelecky´ and J. D. Tasson, “Constraints on Lorentz violation from gravitational Cerenkov radiation,” Phys. Lett. B 749, 551-559 (2015).
11. L. Maccione, A. M. Taylor, D. M. Mattingly and S. Liberati, “Planck-scale Lorentz violation constrained by Ultra-High- Energy Cosmic Rays,” JCAP 0904, 022 (2009).
12. T. Pruttivarasin et al., “A Michelson-Morley Test of Lorentz Symmetry for Electrons,” Nature 517, 592-595 (2015).

Significant contributions to this work have been made by the following people: C. Argüelles, G. H. Collin, J. M. Conrad, T. Katori, A. Kheirandish, and S. Mandalia.

Get our paper here:

arXiv:1709.03434